

Widely tunable extreme UV frequency comb generation

T. J. Pinkert,¹ D. Z. Kandula,^{1,2} C. Gohle,^{1,3} I. Barmes,¹ J. Morgenweg,¹ and K. S. E. Eikema^{1,*}

¹LaserLab Amsterdam, Institute for Lasers, Life and Biophotonics, Vrije Universiteit, De Boelelaan 1081, 1081 HV Amsterdam, The Netherlands

²Present address: Max-Born-Institut, Max-Born-Strasse 2A, 12489 Berlin, Germany

³Present address: Max-Planck-Institut für Quantenoptik, Hans-Kopfermann-Strasse 1, D-85748 Garching, Germany

*Corresponding author: k.s.e.eikema@vu.nl

Received January 19, 2011; revised April 20, 2011; accepted April 20, 2011; posted April 26, 2011 (Doc. ID 141401); published May 26, 2011

Extreme UV (XUV) frequency comb generation in the wavelength range of 51 to 85 nm is reported based on high-order harmonic generation of two consecutive IR frequency comb pulses that were amplified in an optical parametric chirped pulse amplifier. The versatility of the system is demonstrated by recording direct XUV frequency comb excitation signals in He, Ne, and Ar with visibilities of up to 61%. © 2011 Optical Society of America
OCIS codes: 320.7090, 190.2620, 300.6320, 140.7240, 120.3940, 300.6210.

Frequency comb (FC) lasers have become an important tool in many fields of physics, ranging from precision spectroscopy [1,2] to attosecond science [3]. Typical FCs cover only the IR to UV wavelengths due to the availability of laser materials and the use of low-order frequency conversion. Extension of FCs to much shorter wavelengths such as extreme UV (XUV) ($\lambda < 100$ nm) is pursued by several groups through high-harmonic generation (HHG). It has been shown that HHG can result in (to some degree) phase-coherent upconversion of ultrafast pulses. This has been shown for a single amplified pulse [4], an amplified pulse split in two (spatially or temporally) [4,5], and for an infinite FC pulse train enhanced in a resonator cavity [6–8]. Alternatively, phase-coherent amplification of two or more FC pulses in combination with low and high harmonics has been demonstrated as well [9–11], and to the best of our knowledge only in this case could precision metrology in the XUV be shown [11].

In this Letter we demonstrate the versatility and tunability of the method based on FC amplification and upconversion of only two FC pulses by recording XUV FC (XFC) spectroscopic signals over ranges between 51 and 85 nm in He, Ne, and Ar. With two pulses the spectrum still peaks at the positions determined by the modes of the original FC, but now in the form of a cosinelike modulation. The broad “modes” are not limiting the resolution, as the time between the pulses can be increased to reduce the mode distance and therefore increase the resolution (the mode spacing is inversely proportional to the delay of the pulses) [10]. After amplification and HHG in a gas jet, the XUV pulses are used to directly excite a transition in a noble gas. By changing the repetition rate of the FC in the IR, the modes in the XUV are scanned over the transition. This results in a cosinelike excitation spectrum, much like in Ramsey spectroscopy [12].

A schematic of the system can be seen in Fig. 1. The FC delivering the phase-coherent pulses is based on Ti:sapphire, with an average power of 800 mW and a pulse duration of less than 20 fs. The repetition rate ($f_{\text{rep}} = 150$ MHz) and carrier-envelope offset frequency ($f_{\text{CEO}} = 37.5$ MHz) of the FC are referenced to a global-positioning-system-disciplined Rb clock. Amplification of two pulses from the FC takes place in a three-stage noncollinear optical parametric chirped pulse amplifier (NOPCPA). The

pump laser for this system has been designed to produce two 50 ps pulses of ≈ 100 mJ at 532 nm that are delayed carefully to match the time separation of the FC pulses. Two FC pulses, each less than 0.5 nJ in energy and ≈ 2 ps long after the stretcher, are amplified in the NOPCPA system to 5 mJ using two beta barium borate crystals. After recompression in a grating compressor, 1–2 mJ per pulse is available for HHG.

To generate the XFC, the 6.1 mm diameter amplified IR beam is focused with a 50 cm lens into a pulsed noble gas jet (Kr for the fifteenth harmonic, Xe for thirteenth and lower harmonics). Only a single transition should be excited by the XFC, otherwise a reduction in contrast and uncontrolled shifts of the cosine-shaped signal can occur. The transition frequency can be obtained from this signal because a maximum occurs each time the transition comes into resonance with one of the XFC modes centered at $f_m = qf_{\text{CEO}} + mf_{\text{rep}} + \Delta\phi_{\text{eff}}f_{\text{rep}}/2\pi$. In this expression, q is the harmonic order, m is the mode number, and $\Delta\phi_{\text{eff}}$ is an effective differential phase shift at the transition frequency that takes phase shifts in the IR (e.g.,

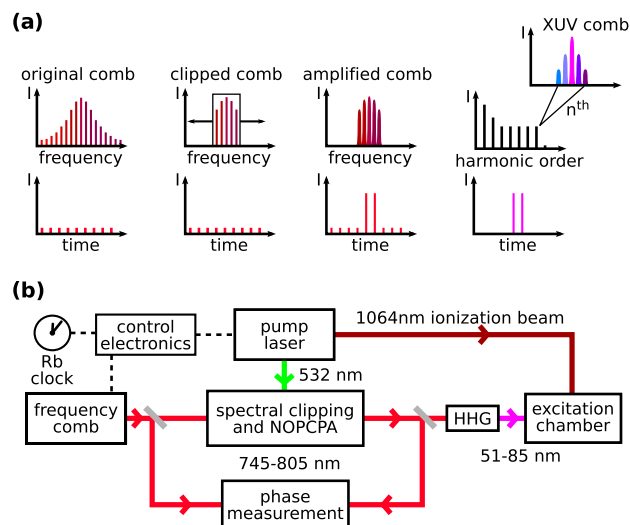


Fig. 1. (Color online) (a) Time and frequency domain structure in the XFC system. From left to right: FC output, spectrally clipped FC, amplified FC, FC after HHG. (b) XFC spectroscopy system, where two FC pulses are amplified in the NOPCPA, upconverted by HHG for direct XFC spectroscopy.

due to the NOPCPA [13]) and the HHG process into account [11]. The XUV bandwidth (the XFC wavelength span, <0.1 nm) is controlled by a slit in the Fourier plane of the stretcher, which limits the amplified spectrum in the IR to 6 nm for the He and Ne spectroscopy and to 3 nm for the Ar spectroscopy. The central XFC wavelength can be coarsely tuned by changing the position of the slit in the stretcher, selecting IR wavelengths between 805 and 740 nm at the fundamental.

The XUV light is crossed perpendicularly with a low-divergence (<3 mrad) pulsed atomic beam. Whenever one of the XFC modes comes into resonance, a peak in the excitation probability occurs. Excited atoms are detected via ionization with a 1064 nm pulse and a time-of-flight mass spectrometer. A channel electron multiplier is used to count the ions, while the XUV intensity of the harmonic used for excitation is measured with a grating monochromator and a photomultiplier.

The tunability of the system at the conditions required for XFC generation is demonstrated first by performing coarse spectroscopy on He, Ne, and Ar with a single up-converted pulse of the FC's pulse train (which does not form a comb). By changing the IR intensity and the gas medium for HHG, the cutoff photon energy is tuned to the harmonic that is used for the spectroscopy (ninth for Ar, thirteenth for Ne, and fifteenth for He). In this way direct ionization due to XUV light of higher harmonic orders is minimized. To record these spectra, the ion signal was measured at each wavelength (with steps of 0.25–1 nm in the IR) for 500 laser shots while scanning the slit in the stretcher. Signal from ionization (10–20%) due to higher HHG orders was measured by blocking the ionization beam and subtracted from the signal.

Figure 2 (bottom) shows these spectra of ground-state transitions in Ar, Ne, and He [the arrows indicate National Institute of Standards and Technology (NIST) database line positions [14] for comparison]. In Ar the transitions to the excited states $3p^5(^2P_{3/2})4d[1/2]_1$ to $3p^5(^2P_{1/2})6s[1/2]_1$ have been recorded. In Ne excitation to $2p^5(^2P_{3/2})5s[3/2]_1$ to $2p^5(^2P_{3/2})7d[3/2]_1$ is shown, and in He the $1snp\ ^1P_1$, $n \in \{4, \dots, 9\}$ series can be distinguished up to $n = 9$. The XUV scanning range was determined at the low-energy side by the requirement that the 1064 nm beam could ionize the excited state.

To generate an XFC, a second amplified and up-converted pulse was added and care was taken that the HHG process did not saturate ($I_{\text{IR}} < 5 \cdot 10^{13}$ W/cm² for Kr, and a factor of 2 lower for HHG in Xe). In this manner two phase-coherent XUV pulses are produced, leading to a cosine-modulated spectrum. The mode spacing in the XUV remains the same as that of the original FC in the IR, which was close to $f_{\text{rep}} = 150$ MHz. Given the XUV spectral width, there are approximately $2.8 \cdot 10^4$ – $8.0 \cdot 10^4$ XFC modes present for a central wavelength of 85–51 nm. The slit in the stretcher was used to select a particular transition, and the repetition rate of the FC in the IR was then scanned to move the comb modes over the transition. Figure 2 (top) shows this XFC signal recorded for selected transitions in He, Ne, and Ar. The signal (based on approximately 20,000–40,000 laser shots, binned into 20 groups per XFC excitation signal period) is normalized to the measured average XUV intensity.

In [11] we demonstrated that, from the XFC signal in He (similar to that shown in Fig. 2), the transition frequencies can be obtained with up to 6 MHz accuracy at 51 nm. For the wavelength range presented here in Ar and Ne, at least a similar accuracy can be obtained experimentally, as all the systematic and statistical errors are expected to be smaller. However, a comparison with theory is hampered by a lack of sufficiently accurate calculations in Ne and Ar. Therefore, we concentrate in this Letter on the tunability and contrast (defined as the signal amplitude over the average) of the XFC signal. This contrast is mostly influenced by Doppler broadening, lifetime of the excited state relative to the pulse delay, background from direct ionization by higher harmonics, and phase noise introduced in the NOPCPA (typically tens of milliradians in the IR) and HHG. Phase shifts common to both pulses do not lead to a shift in the mode spectrum or to contrast reduction. However, a differential phase shift, $\Delta\phi$, changes the frequency of the modes according to $\Delta f = f_{\text{rep}} \Delta\phi / (2\pi)$. HHG introduces an IR intensity-dependent adiabatic phase shift in the emitted harmonics [15,16], and accompanying ionization can also lead to phase shifts as large as 2 rad [11]. Because of these effects, phase noise due to variations in IR intensity, pulse intensity ratio, and HHG medium density can reduce the contrast of the measured comb modulation. Doppler broadening is reduced for He in the supersonic atomic

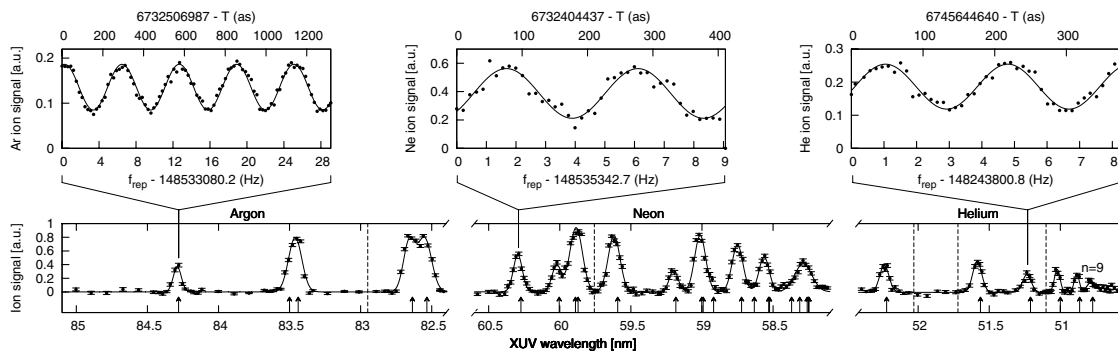


Fig. 2. (bottom) Single-pulse and (top) double-pulse XFC spectra of Ar, Ne, and He. The wavelength axis calibration (bottom) is obtained with an Ando AQ6315A spectrometer in the IR (accurate to 0.03–0.06 nm). The vertical dashed lines indicate separate measurements sessions, while the arrows indicate NIST database line positions [14] for comparison. (top) XFC signal measured on the Ar $3p^5(^2P_{3/2})4d[1/2]_1$ (contrast $\approx 37\%$), Ne $2p^5(^2P_{3/2})5s[3/2]_1$ (45%), and He $1snp$ (36%) state by scanning f_{rep} of the FC. For He a mixture with Ne was used to reduce Doppler broadening to 40 MHz.

beam by mixing it with Ne and Ar, leading to a He velocity of 830(200) m/s and 500(250) m/s, respectively [11].

The highest XFC signal contrasts (averaged over several measurements) were seen in He (55% when seeded in Ar) and Ar (61%), while for Ne a contrast of 43% was observed. Measurements on one transition varied up to 10% in contrast. We use a model assuming a Gaussian shape XUV phase noise and Doppler profile to obtain an estimation for the atomic beam divergence and XUV jitter from the measurements. This results in an atomic beam divergence of 2.4 mrad (FWHM) and an XUV phase jitter of 0.40(13), 0.46(9) and 0.41(10) cycles for the He, Ne, and Ar measurements, respectively. For He almost a factor of 2 lower XUV phase noise is expected based on the stability of the FC (1.6 MHz mode line width) and NOPC-PA pulse energy stability (6% rms). For Ar measurements, even lower XFC noise is expected due to the lower harmonic (ninth compared to fifteenth for He). No clear correlation between the contrast and IR intensity, intensity jitter, or harmonic order is observed in the measurements, which might indicate an underestimation of the influence of density variations in the HHG jet or of the bandwidth of the FC modes in the IR.

In conclusion, we have demonstrated widely tunable (51–85 nm) XUV comb generation and spectroscopy based on amplification and upconversion of two FC laser pulses. With the present setup, continuous tuning down to 47 nm is possible, and with higher harmonics even 25 nm should be feasible with >10% contrast. However, the latter has not been tested due to a lack of suitable transitions. A submegahertz accuracy should become possible by employing pulses with a bigger time separation, combined with further Doppler broadening reduction using, e.g., a two-photon transition.

This work was supported by the Foundation for Fundamental Research on Matter through its Industrial Partnership Programme “Metrology with Frequency Comb Lasers;” by the Netherlands Organisation for Scientific Research through a Vici grant; by the European Union (EU) via the Seventh Framework Programme, Joint

Research Activity, Attosecond Laser sources and Applications, Design and Innovation; and by the Humboldt Foundation.

References

1. R. Holzwarth, T. Udem, T. W. Hänsch, J. C. Knight, W. J. Wadsworth, and P. S. J. Russell, *Phys. Rev. Lett.* **85**, 2264 (2000).
2. S. A. Diddams, D. J. Jones, J. Ye, S. T. Cundiff, J. L. Hall, J. K. Ranka, R. S. Windeler, R. Holzwarth, T. Udem, and T. W. Hänsch, *Phys. Rev. Lett.* **84**, 5102 (2000).
3. F. Krausz and M. Ivanov, *Rev. Mod. Phys.* **81**, 163 (2009).
4. M. Bellini, C. Lyngå, A. Tozzi, M. B. Gaarde, T. W. Hänsch, A. L’Huillier, and C.-G. Wahlström, *Phys. Rev. Lett.* **81**, 297 (1998).
5. I. Liotos, S. Cavalieri, C. Corsi, R. Eramo, S. Kazianis, A. Pirri, E. Sali, and M. Bellini, *Opt. Lett.* **35**, 832 (2010).
6. C. Gohle, T. Udem, M. Herrmann, J. Rauschenberger, R. Holzwarth, H. A. Schuessler, F. Krausz, and T. W. Hänsch, *Nature* **436**, 234 (2005).
7. R. J. Jones, K. D. Moll, M. J. Thorpe, and J. Ye, *Phys. Rev. Lett.* **94**, 193201 (2005).
8. D. C. Yost, T. R. Schibli, J. Ye, J. L. Tate, J. Hostetter, M. B. Gaarde, and K. J. Schafer, *Nat. Phys.* **5**, 815 (2009).
9. S. Witte, R. T. Zinkstok, W. Hogervorst, and K. S. E. Eikema, *Opt. Express* **13**, 4903 (2005).
10. R. T. Zinkstok, S. Witte, W. Ubachs, W. Hogervorst, and K. S. E. Eikema, *Phys. Rev. A* **73**, 061801 (2006).
11. D. Z. Kandula, C. Gohle, T. J. Pinkert, W. Ubachs, and K. S. E. Eikema, *Phys. Rev. Lett.* **105**, 063001 (2010).
12. N. F. Ramsey, *Phys. Rev.* **76**, 996 (1949).
13. D. Z. Kandula, A. Renault, C. Gohle, A. L. Wolf, S. Witte, W. Hogervorst, W. Ubachs, and K. S. E. Eikema, *Opt. Express* **16**, 7071 (2008).
14. Y. Ralchenko, A. E. Kramida, J. Reader, and NIST ASD Team, “NIST Atomic Spectra Database,” version 3.1.5 (National Institute of Standards and Technology, 2008), retrieved August 25, 2010, <http://physics.nist.gov/asd3>.
15. M. Lewenstein, P. Balcou, M. Y. Ivanov, A. L’Huillier, and P. B. Corkum, *Phys. Rev. A* **49**, 2117 (1994).
16. C. Corsi, A. Pirri, E. Sali, A. Tortora, and M. Bellini, *Phys. Rev. Lett.* **97**, 023901 (2006).